Int. J. Electrochem. Sci., 9 **(2014)** 4297 - 4314

International Journal of
ELECTROCHEMICAL
SCIENCE
www.electrochemsci.org

Nanostructured ZnO, ZnO-CeO_2, ZnO-Cu_2O Thin Films Electrodes Prepared by Electrodeposition for Electrochemical Degradation of Dye

M. El Hajji[1], *A. Hallaoui*[1], *L. Bazzi*[1], *A. Benlhachemi*[1], *O. Jbara*[2,*], *A.Tara*[2], *B.Bakiz*[1,3]

[1] Materials and Environment Laboratory, Faculty of Sciences, Agadir, Morocco.
[2] Engineering and Materials Science Laboratory (LISM), UFR Sciences, University of Reims, France.
[3] Microelectronic Materials and Nanosciences Institute of Provence, CNRS UMR 7334, University South Toulon-Var, France.
[*]E-mail: omar.jbara@univ-reims.fr

Received: 24 March 2014 / *Accepted:* 28 April 2014 / *Published:* 19 May 2014

Here, we report that thin films of ZnO, ZnO-Cu_2O and ZnO-CeO_2 nanocomposite oxides, can be successfully synthetized by electrochemical deposition route. This path represents a simple, quick and economical method for a controllable growth. Aqueous zinc nitrate for ZnO, copper or cerium nitrates solutions for ZnO-Cu_2O and ZnO-CeO_2 were used. Structural and morphological properties of both electrodeposited ZnO, ZnO-Cu_2O and ZnO-CeO_2 were carried out using X-ray diffraction and scanning electron microscopy (SEM). The morphology and size of the thin films can be tailored by optimizing the synthetic parameters. The thin films obtained were tested as electrodes and their electrocatalytic properties were compared.

Keywords: Thin films, ZnO, ZnO-CeO_2, ZnO-Cu_2O, Electrochemical Deposition.

1. INTRODUCTION

Zinc oxide « ZnO » is a semiconductor with wide direct band gap (3.37 eV) [1], which has many interesting properties (chemical [2-4], photo-catalytic [5-9], piezoelectric and optical [10-14]). A wide range of applications of ZnO oxide such as laser diodes [15] piezoelectric transducers [10], transistors [16], phosphors [17], a transparent buffer layer in copper indium gallium solar (CIGS) diselenide cell devices [18], makes it one of the most studied in the last decade, particularly in the field of nanostructured materials. ZnO can be grown by different methods such as electrodeposition [19-21], which has low equipment and production cost and is simple to operate. Electrodeposition also has the

advantage of having low temperature processing, allows various substrate shapes and controllable film thickness. Under normal laboratory conditions, this technique also avoids the use of vacuum systems, which allows nanomaterials growth [22].

In this work, we investigated the electrochemical synthesis of thin films of pure ZnO, ZnO-Cu_2O and ZnO-CeO_2 nanocomposite oxides on several substrates. Properties and electrochemical deposition of these thin films will be compared in order to assess the quality of electrodeposited nanocomposite oxides used later as material of electrode for the degradation of organic contaminants, especially the dyes.

2. EXPERIMENTAL

For all the developed thin films, the deposition conditions are given below. Stainless steel, aluminum and titanium substrates were used as working electrode. Prior to the deposition, substrates were polished mechanically using a mechanical polishing machine on a paper of polishing SiC 800, 1200 and SiC 2000 for the completion. Then the substrates were washed thoroughly with distilled water, rinsed with acetone, and cleaned with ethanol. Finally, they were dried with pulsed hot air immediately before the deposition. XRD analysis was carried out using a BURKER SIEMENS D5000, with Cu Kα1 source (λ = 1.5406 Å) at a glancing angle of 0.5°. To study the surface morphology of obtained films, SEM observation was carried out using Philips XL 30 ESEM-Field-Emission Gun.

2.1. Electrodeposition of zinc oxide

ZnO thin films were electrodeposited potentiostatically using a conventional three electrode system, with platinum sheet counter electrode and saturated calomel electrode « Hg/ Hg_2Cl_2/ KCl »« +242 mV vs normal hydrogen electrode at room temperature » reference electrode.

PGP 201 Radiometer Copenhagen Voltalab.TM potentiostat/galvanostat was employed to perform the potentiostatic deposition. The aqueous solution contained 0.5 M zinc nitrate, Zn $(NO_3)_2$•$6H_2O$ dissolved in 200 ml bidistilled water. The temperature was maintained at 65°C (± 2°C). Samples with an effective surface area of 1.7cm^2 were grown at various cathodic intensities in front of 3 and 9mA/cm^2 vs SCE to study various properties. In this context, the same conditions to deposit ZnO-Cu_2O and ZnO-CeO_2 nanocomposite oxides were adopted. The thickness of electrodeposited ZnO onto stainless steel, aluminum and titanium substrates was controlled. Some electrodeposited films of ZnO were annealed for 30 minutes at 45O°C.

2.2. Electrodeposition of ZnO-CeO_2

In this part, stainless steel substrate was used as working electrode. The following chemical products used to prepare the thin films of ZnO-CeO_2 nanocomposite were: 0.5M zinc nitrate, $Zn(NO_3)_2$•$6H_2O$, like zinc precursor, 0.05M cerium nitrate pentahydrated, $Ce(NO_3)_3$,$6H_2O$ (delivered

by the company Alpha Aeosos) like cerium precursor, and 1M potassium nitrate « KNO_3 » like electrolyte support. The pH of the electrolytic bath was 4.6.

2.3. Electrodeposition of ZnO-Cu_2O

ZnO-Cu_2O was electrodeposited onto stainless steel substrate using the following chemical products: 0.5 M zinc nitrate, $Zn(NO_3)_2 \bullet 6H_2O$, like zinc precursor, 0.05 M copper nitrate, $Cu(NO_3)_2$,$3H_2O$ (delivered by the company Alpha Aeosos) like copper precursor, and 1 M potassium nitrate « KNO_3 » like electrolyte support. The pH of the solution was adjusted with KOH.

2.4. Electrocatalytic activity experiment and conditions

The Electrochemical analysis was performed using the same *Potentiostat/ Galvanostat* used for the electrodeposition. A conventional three electrodes cell (100 cm^3) thermoregulated glass cell was used. The anode was the as-prepared thin films such (ZnO-CeO_2)/Ti, (ZnO-Cu_2O)/Ti, and ZnO/Ti, whereas the cathode was a platinum electrode and the gap between electrodes was 1cm. A saturated calomel electrode (SCE) was used as a reference.

Thereafter, a comparative study was executed using these anodes. Seventhly milliliters of synthetic wastewater containing 20 mg/L MB and 2% NaCl were charged in the electrolysis cell. The NaCl was added as a supporting electrolyte. The cell was connected to a water bath in order to control and keep the temperature constant at 30°C. It was set on a magnetic stirrer for continuous mixing. The operating current density during degradation of MB was 9$mAcm^{-2}$. The degradation took 90 minutes.

The UV adsorbency spectrogram at wavelengh range 400-800 nm was recorded using a *TU1800-UV-vis spectrometer*. *LOVIBOND Checkit COD VARIO* device was used for all mesures of COD. The samples were taken during electrolysis with various time intervals. The rate of mineralization was expressed as a percentage of COD. This rate was given for various reaction times by this relation:

$$\%COD = [(CODi - CODt)/ CODi] * 100$$

With:

- CODi : value of COD (mg/L of O_2) at initial moment
- CODt : value of COD (mg/L of O_2) at t moment

3. RESULTS

3.1. Structural characterization and grain sizes

The XRD studies had been carried out on ZnO, annealed ZnO and two types of nanocomposite zinc oxides in order to determine phase and crystallographic analysis. All XRD patterns obtained were analyzed using the X'Pert HighScore software. Typical X-ray diffractograms of electrodeposited ZnO onto stainless steel substrate before and after heat treatment are shown in fig 1a and 1b, respectively.

The diffractograms show the material to be polycrystalline with hexagonal wurtzite phase. A strongest peak is along the (101) plane. The peaks of annealed ZnO are intense.

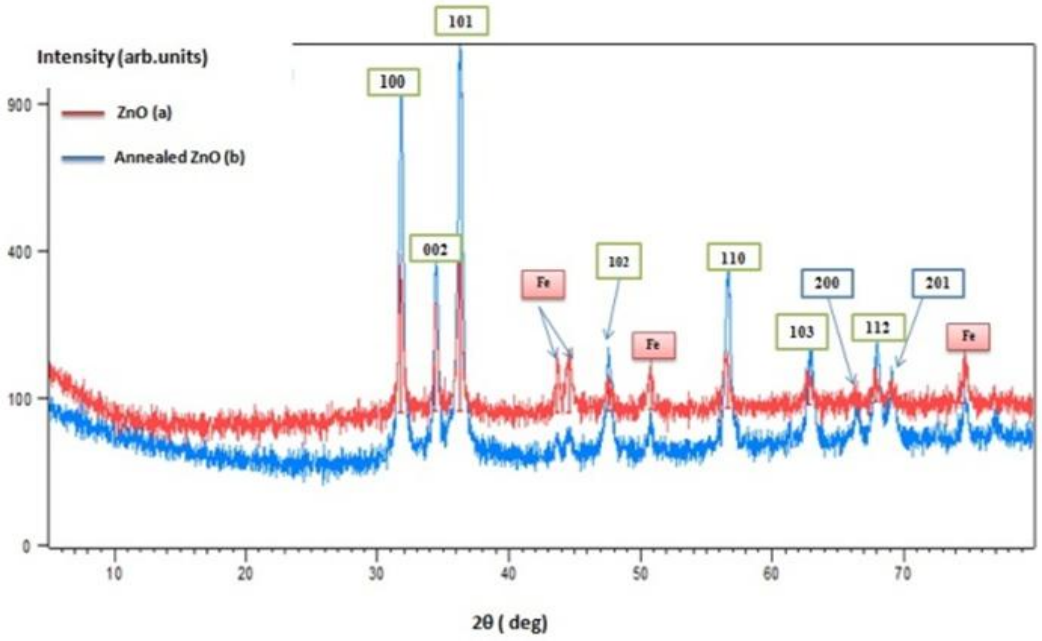

Figure 1. X-ray diffractograms of (a) electrodeposited ZnO and (b) annealed ZnO at 450°C for 30 mn.

To study the effect of changing the current density and the concentration of zinc nitrate we had electrodeposited ZnO onto titanium and aluminum substrates respectively. In this way, we also study the effect of changing the substrate. The results are shown in fig 2 and fig 3.

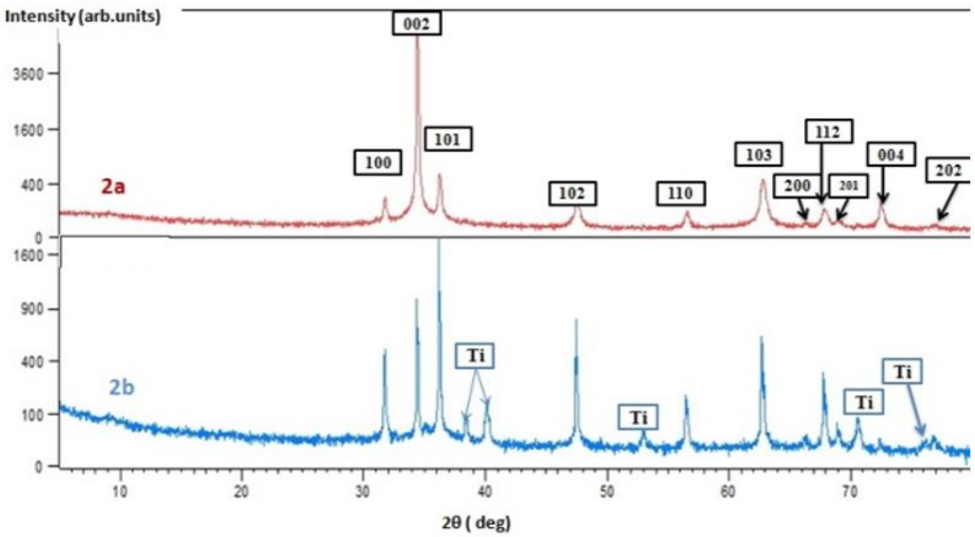

Figure 2. XRD spectra of (a) electrodeposited ZnO « Zn^{2+} = 0.1M » and (b) « Zn^{2+} = 0.5M » onto Ti substrate at j= -3mA/cm^2.

In the XRD spectra « fig 2a » the characteristic peaks of Ti substrate are absent. These spectra show the material to be polycrystalline and a strongest peak corresponding to the (002) plane appeared. These results are completely the opposite of those given in fig 2b. The effect of changing the concentration of zinc nitrate clearly appears. Generally, ZnO keep its hexagonal wurtzite phase. Fig.3 shows the XRD spectra of electrodeposited ZnO onto aluminum substrate.

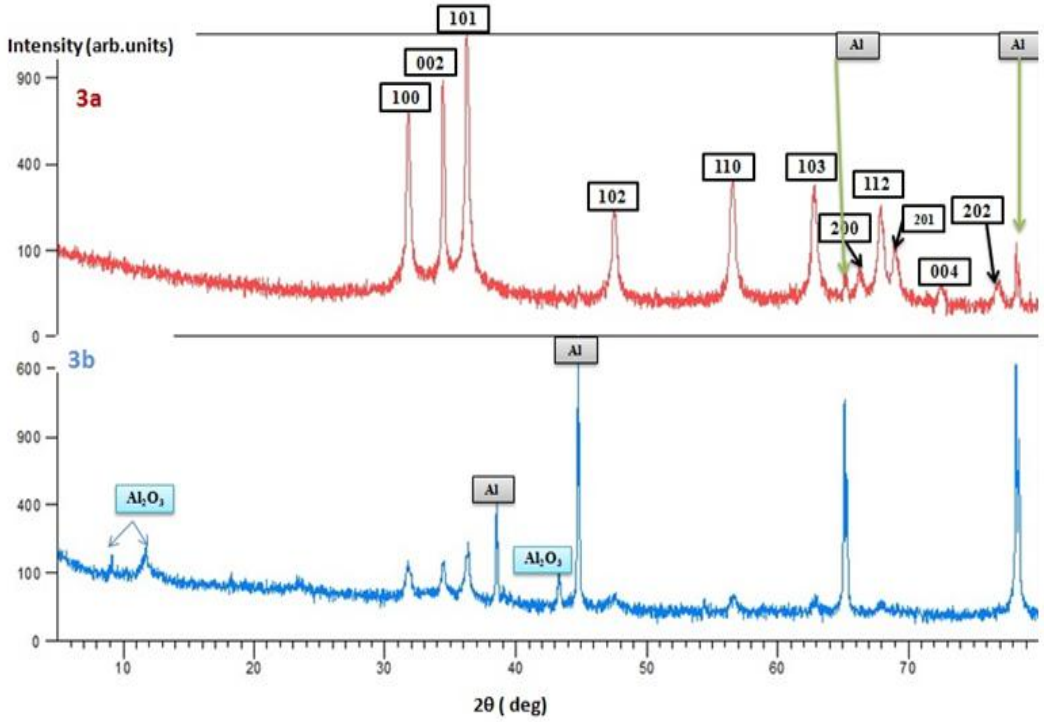

Figure 3. XRD spectra of electrodeposited ZnO (a) j= -3 mA/cm^2 and (b) j= -9 mA/cm^2 on Al substrate.

The used concentration of zinc nitrate was 0.5 M. From Fig 3a, the peaks located at 2θ = 31.7°, 34.4°, 36.2°, 47.4°, 56.5°, 62.7°, 66.2°, 67.8°, 68.9°, 72.5°and 76.8° could be related to the (100), (002),(101), (102), (110), (103), (200), (112), (201), (004) and (202) reflections of the zinc oxide species, respectively. These peaks are generally intense. Two peaks related to aluminum substrate appeared in both spectra.

The difference between fig 3a and 3b was due to the current density used. This density had a significant effect on crystallite size. In both cases the diffractogram shows the material to be polycrystalline with hexagonal wurtzite phase and a strongest peak is along the (101) plane. Table.1. shows the calculated average size of the crystallites of electrodeposited ZnO onto stainless steel « SS », aluminum « Al » and titanium « Ti » substrates. The grain sizes estimated from the X-ray diffraction peak width, using Scherrer's formula [23] were between 22 and 50 nm. This result confirms the good crystallinity of the samples and the nanometric size of crystallites.

Table 1. Average size of crystallites of pure ZnO

Substrate	Concentration of Zinc nitrate	Current Density mA/cm^2	Plane direction	Crystallite size D (in nm)
SS	0.5 M	3 mA/cm^2	(101)	40.06
SS/ Annealed ZnO	0.5 M	3 mA/cm^2	(101)	28.06
Al	0.5 M	3 mA/cm^2	(101)	50.8
Al	0.5 M	9 mA/cm^2	(101)	22.6
Ti	0.5 M	3 mA/cm^2	(101)	46
Ti	0.1 M	3 mA/cm^2	(002)	41.1

Fig.4 shows the XRD spectra of the ZnO-CeO_2 deposited onto stainless steel substrate.

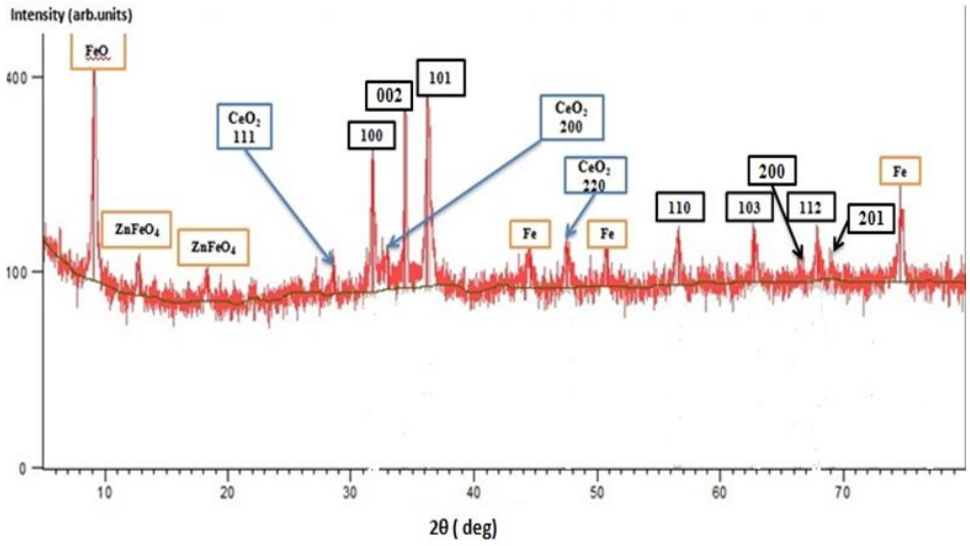

Figure 4. X-ray diffractogram of electrodeposited nanocomposite ZnO-CeO_2 oxides onto stainless steel substrate.

From Fig.4, ZnO has a hexagonal wurtzite phase. A strongest peak is along the (101) plane. The main diffraction peaks of the stainless steel and its appeared oxides « FeO, $ZnFeO_4$ » are located at 2θ = 9.13°, 12.75°, 18.31°, 44.56°, 50.76°and 74.64°. For ceria « CeO_2 », three peaks located at 2θ = 28.58°, 32.95° and 47.52° are investigated. Generally, ZnO phase was the major compound diffracting from the deposit, and no diffraction line associated with Ce (III) hydroxide was present. The XRD spectrum of electrochemical deposition of ZnO-Cu_2O nanocomposite oxides onto stainless steel substrate is shown in fig.5. The peaks of stainless steel substrate are intense. The peaks located at 2θ = 31.8°, 34.5°, and 36.4° could be related to (100), (002), (101) reflections respectively of ZnO species which are generally less intense. ZnO has a hexagonal wurtzite phase and a strongest peak is along the (101) plane. Three other peaks related to copper (I) oxide Cu_2O are observed.

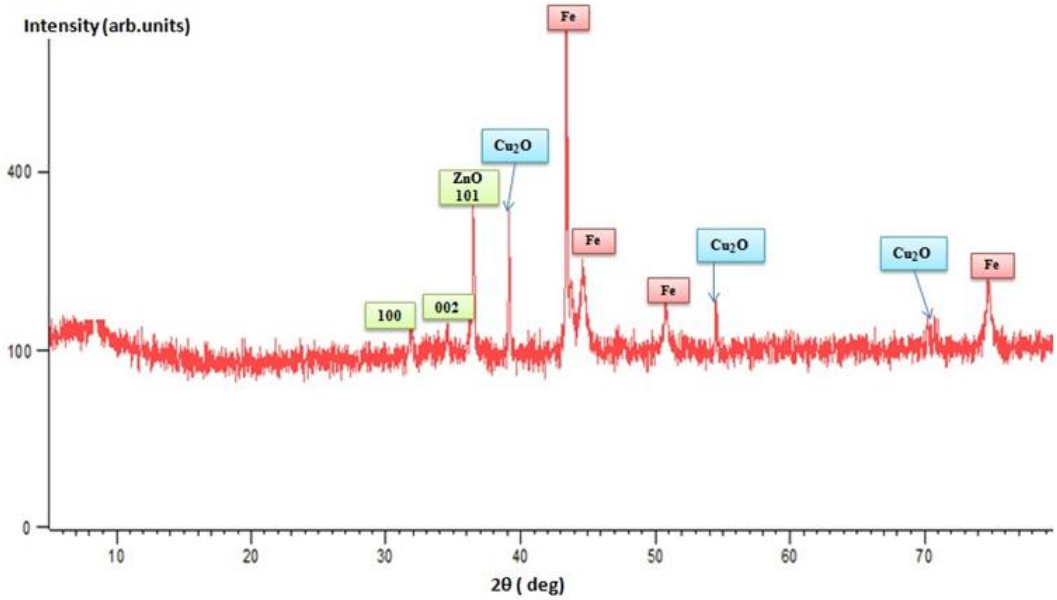

Figure 5. Typical XRD spectra of electrodeposited ZnO-Cu_2O

Crystallites size of electrodeposited ZnO-Cu_2O and ZnO-CeO_2 nanocomposite oxides on stainless steel substrate were calculated using a Scherrer equation [23]. Table.2 shows the results obtained. The computed value of crystallites size of these samples is between 32 and 111 nm. Thus, compared with the results of pure ZnO « Table.1. », grain sizes of ZnO show an increase after introducing cerium and copper.

Table 2. Crystallites size of thin films of ZnO-CeO_2 and ZnO-Cu_2O

Nanocomposite oxides	Oxide-Type	Crystallites size D (in nm)
ZnO-CeO_2	ZnO	51.4
	CeO_2	32.2
ZnO-Cu_2O	ZnO	78.9
	Cu_2O	111.4

3.2. Surface morphology

SEM observation was used to investigate the surface morphology. Fig.6 illustrates the appearance of the electrodeposited ZnO onto stainless steel substrate showing homogeneous and void-free surface.

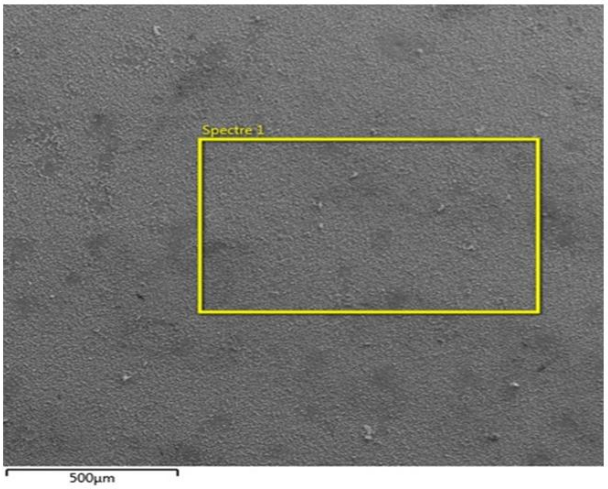

Figure 6. SEM micrograph of electrodeposited ZnO

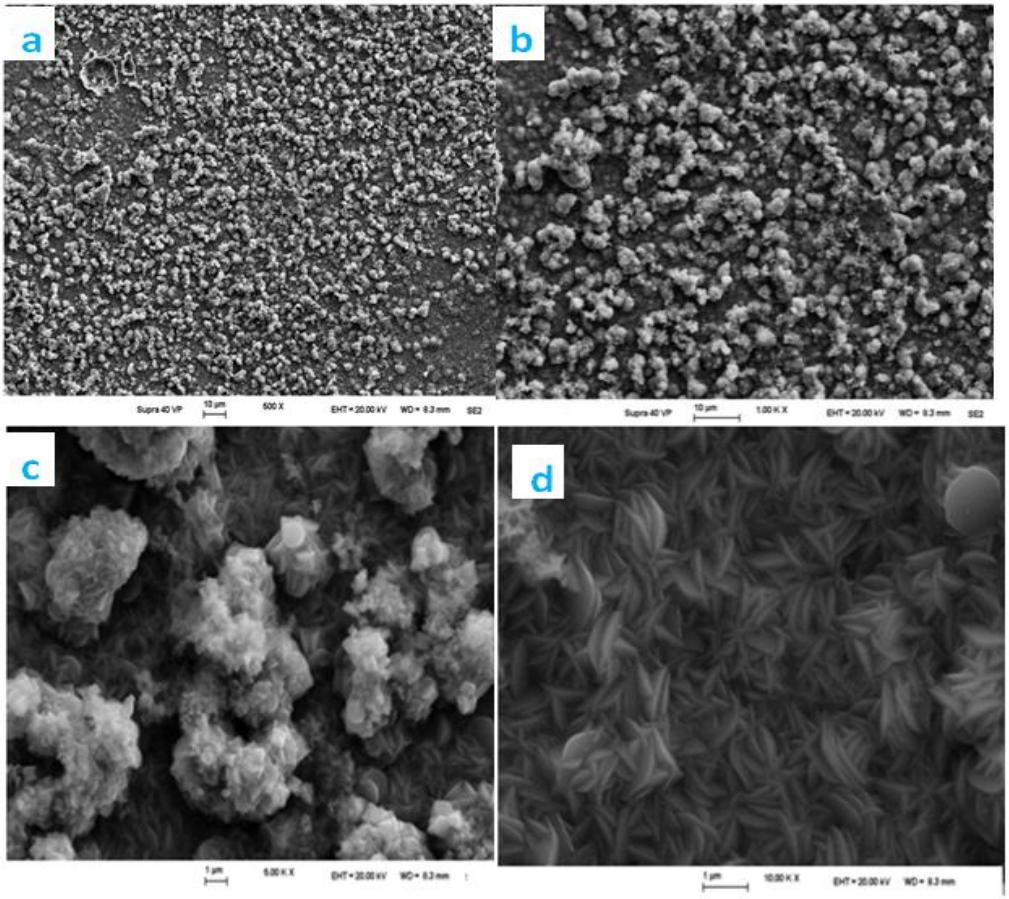

Figure 7. Typical SEM images of thin films grown on SS substrate at different magnifications

Fig.7 shows the SEM images of the ZnO deposit obtained using different magnification. Generally, the products were observed as nanostructures with diameters of a few tens of nanometers on the substrate. The length of nanostructures is up to a few micrometers. The films are compact, have a dense structure, and the grains are larger or at least thicker « Fig.7.a and Fig.7.b ».

The enlargement of an area allows us to view that the layers obtained had a specific morphology made up of micrometric agglomeration of grains with a different homogeneous sizes « Fig.7.c ». In Figure 7.d. the surface of this layer presents the asperities of very small size. They make the appearance of the layer very rough coating.

SEM provides information not only on morphology, the distribution and the size of the grains or the agglomerates, but also on the local chemical composition when it is coupled with EDS X-Ray spectrometer. Fig.8 shows the results got by EDS X-Ray analysis on thin films of pure zinc oxide.

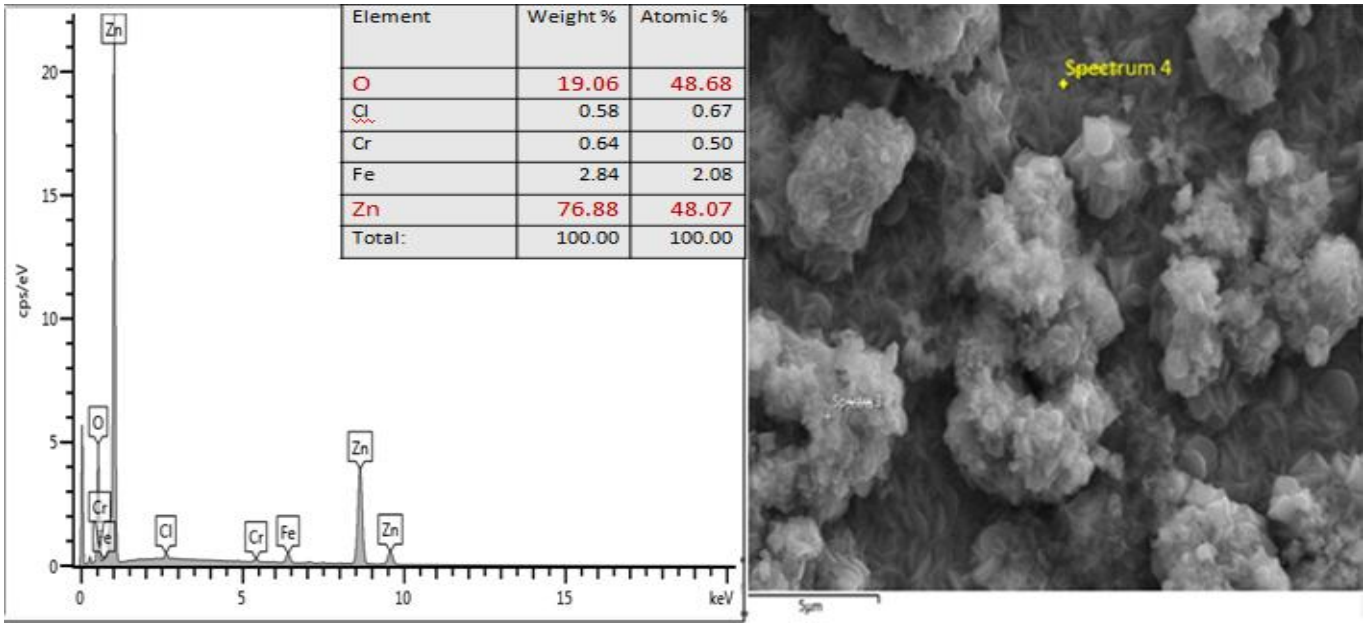

Figure 8. EDS spectrum (left) related to the deposit of the pure zinc oxide. The SEM image (right) indicates the zone where the spectrum is acquired.

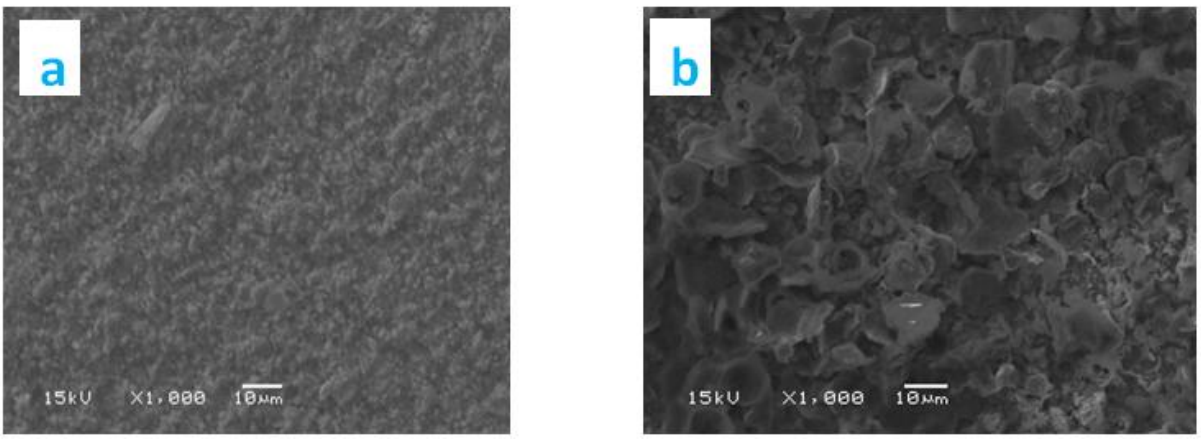

Figure 9. SEM images of deposits made on Al substrate with a fixed intensity - 3mA/cm^2 (a) and - 9mA/cm^2 (b).

The oxygen and zinc elements are well present. The semi-quantitative EDS analysis shows that the ratio [Zn] / [O] is slightly lower than 1. This indicated that the deposit had slightly excess of oxygen. However, the percentage of zinc and oxygen are close to the nominal composition.

Fig.9 shows the deposits of ZnO on Al substrate. The texture evolution of deposits and grain size as a function of current density used is in good agreement with the predictions of XRD analysis. It is important to note that deposits made on various metal surfaces have quite different microstructures depending on the nature of the substrate used. Fig.10. illustrates the results obtained.

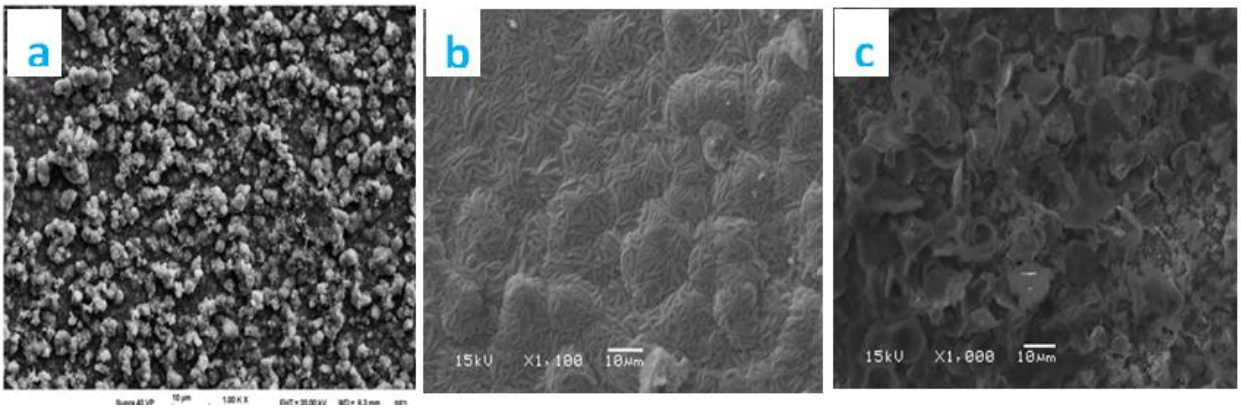

Figure 10. SEM micrographics of the electrodeposited pure ZnO thin film on (a) SS (b) Ti and (c) Al substrates.

The surface of electrodeposited ZnO thin films on SS substrate (Figure.10.a) presents asperities of very small size, the deposits formed onto Ti substrate (Figure.10.b) have a surface composed of elongated grains shapes while the deposits made on the Al substrate (Figure.10.c) have a surface consisting of platelet shape grains.

Fig.11. shows the SEM surface morphology of ZnO-CeO_2 nanocomposite oxides deposited at -3 mA/cm^2 current density onto SS substrate.

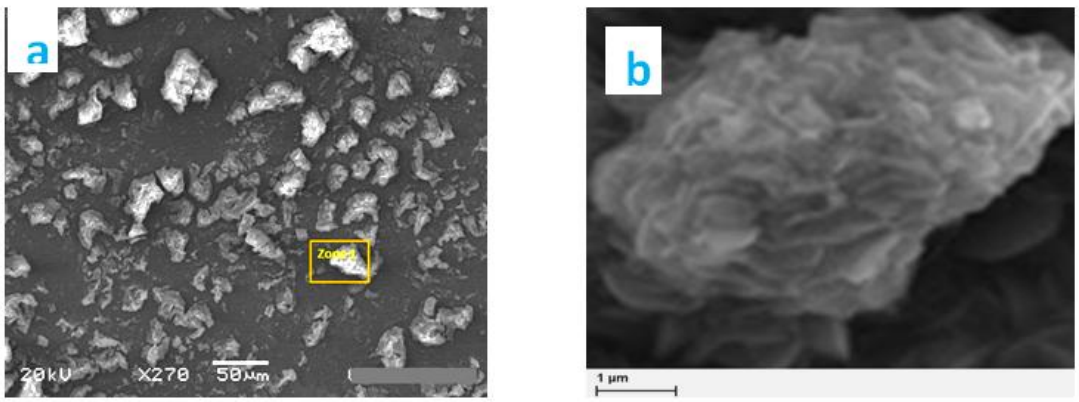

Figure 11. SEM micrographics for the deposits of ZnO-CeO_2 (left) and a zoom of boxed area (right)

The thin films obtained have a specific morphology made up of « nano-micrometric » heterogeneous grains of different sizes. The enlargement of boxed area « Fig.11.b » makes it possible to view a cluster of grains of micrometric size. However, an important network of cracks appears in the deposit. As discussed in the literature [24,25], generally, these cracks usually appear during the electrodeposition of ceria.

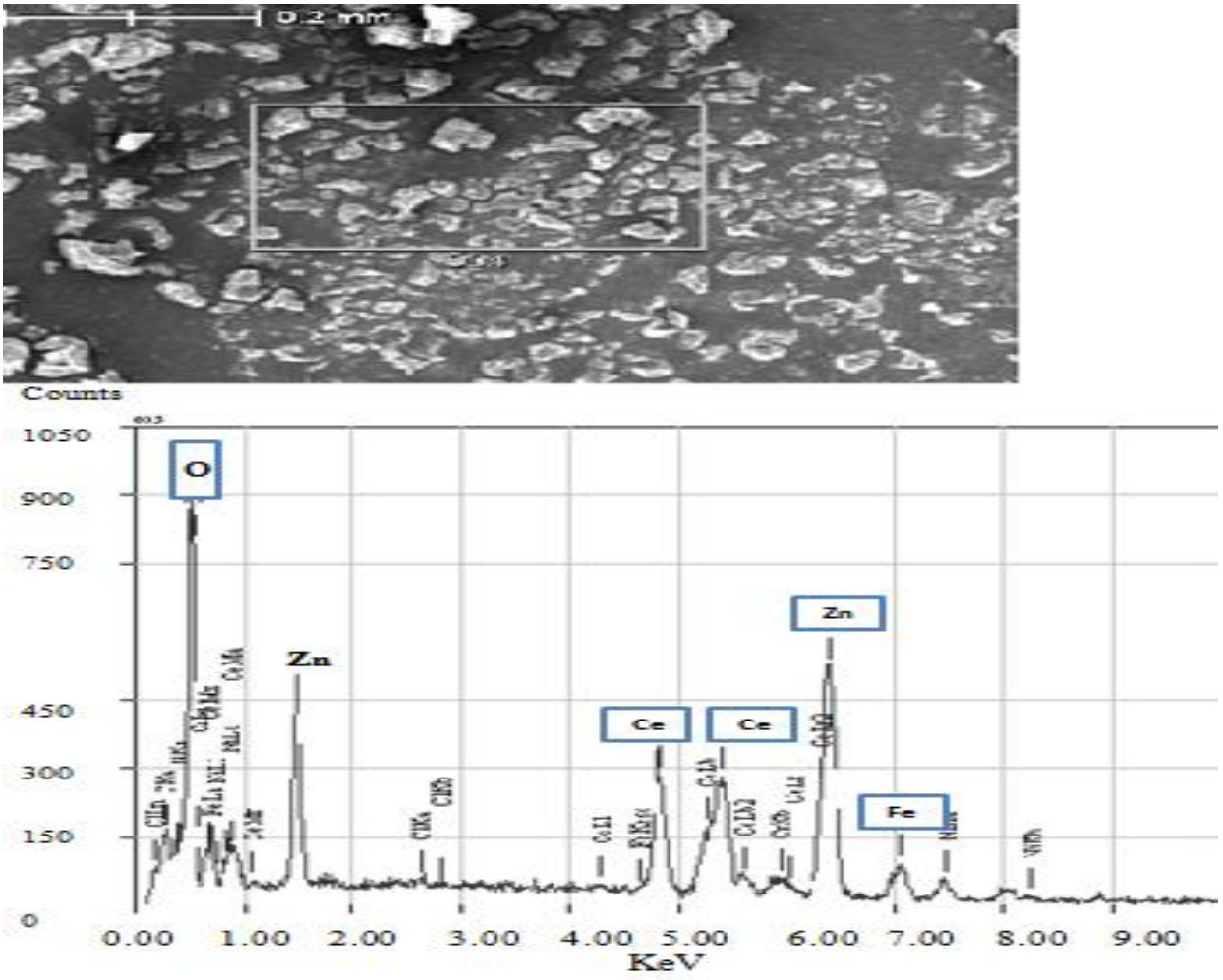

Figure 12. EDS Spectrum (bottom) of ZnO-CeO_2 in the boxed area (top) of SEM image (fig.11.a)

Fig.12 shows the results got by EDS analysis that confirms the presence of oxygen, zinc and ceria elements in the deposit.

Fig.13. shows the SEM images of surface morphology of electrodeposited ZnO-Cu_2O nanocomposite oxides onto SS substrate. Fig.13.a presents an image of large area of the surface of the deposit that shows a homogenous morphology without cracks. From Fig.13.b and Fig.13.e, the increase of magnification allows visualizing of a cluster of small grains of nanometric size and show that the morphology of cuprite « Cu_2O » is similar to a cauliflower shape. In addition, the film is compact and have a dense structure.

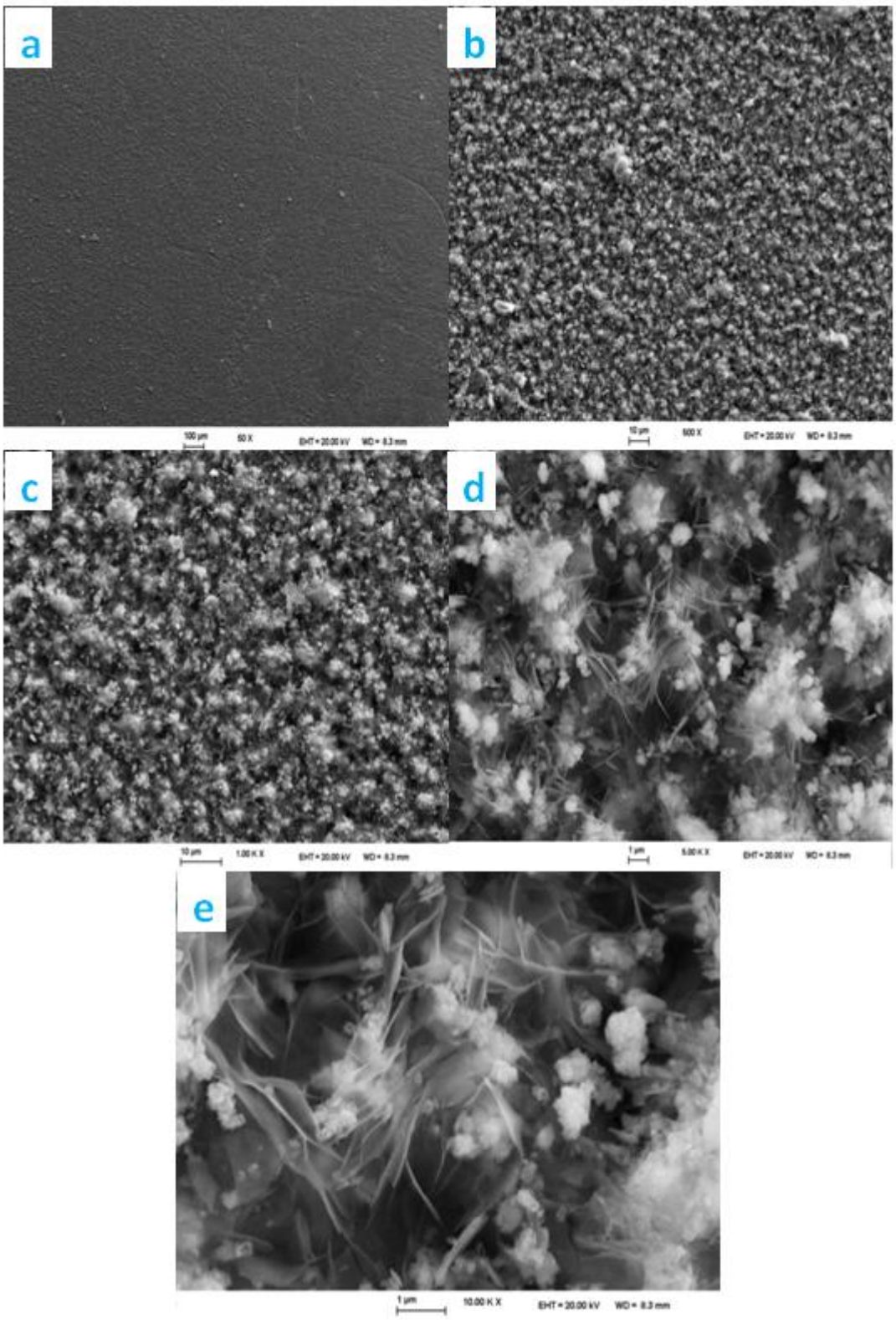

Figure 13. SEM micrographs for electrodeposited ZnO-Cu_2O nanocomposite oxides at different magnification

Fig.14 presents the results got by EDS analysis concerning the thin films of ZnO-Cu_2O nanocomposite oxides. These results show that the agglomerates of grains in the film contain zinc, copper and oxygen. The low percentage of the compounds of the steel observed in the spectra

corresponds to the contribution of the substrate excited by incident electrons after crossing the film. The total analysis confirms the nominal composition.

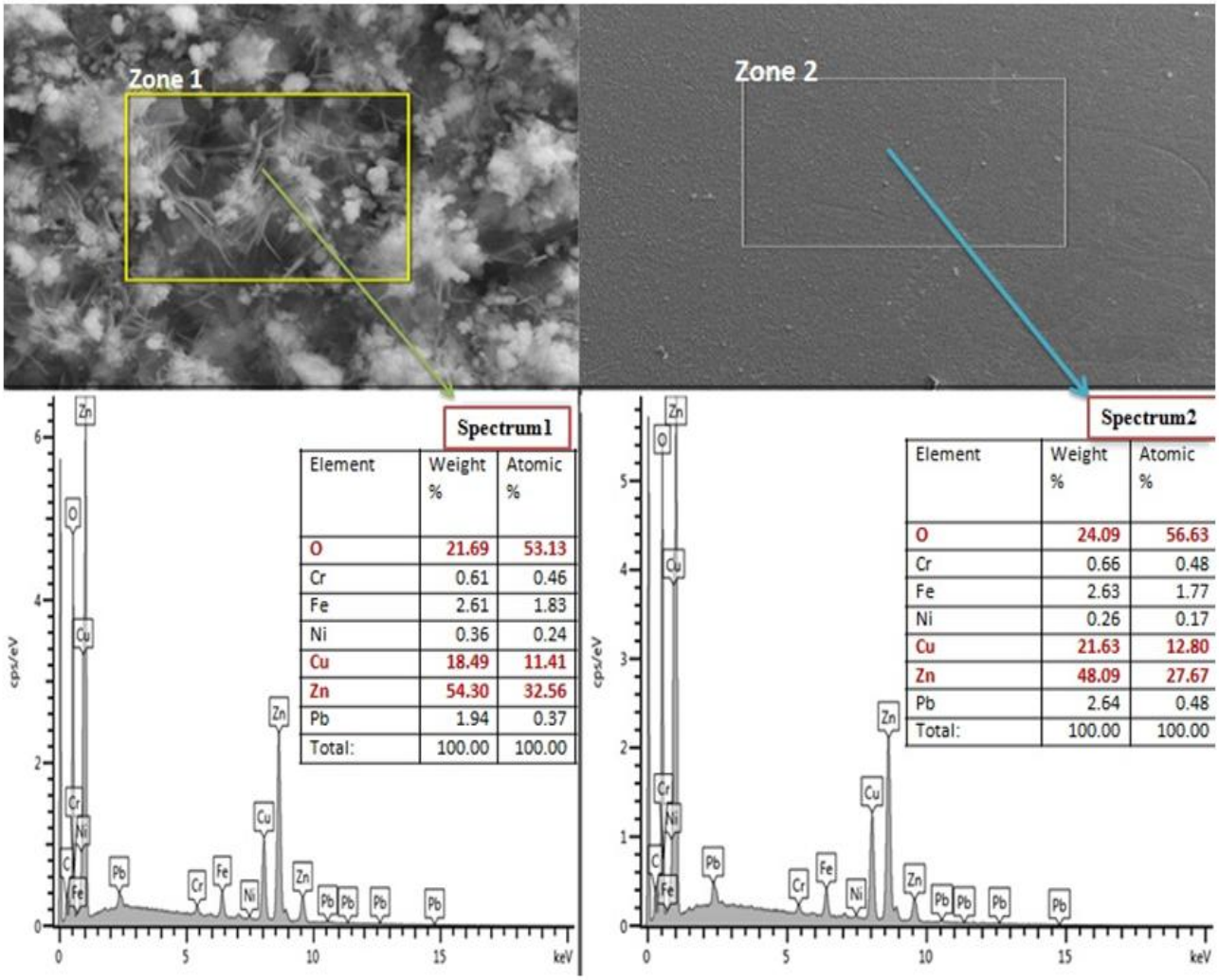

Figure 14. EDS spectra of ZnO-Cu_2O nanocomposite (bottom) and the SEM images of their emission area (top)

3.3. Test of electrocatalytic activity of ZnO and its nanocomposites thin films elaborated on stainless steel substrate

The electrocatalytic studies have been carried out to determine the electrolytic efficiency of electrodeposited ZnO-CeO_2 and ZnO-Cu_2O nanocomposite oxides.

From the physicochemical characteristics of methylene blue « MB » used as a reference in the field of dye degradation, this study meets the following selection criterions: its high solubility in water, its pressure, and its easy analysis by UV / vis. Fig 12 shows the spectrum of methylene blue obtained at natural pH (5.9) and diluted in medium «10^{-5} M ».

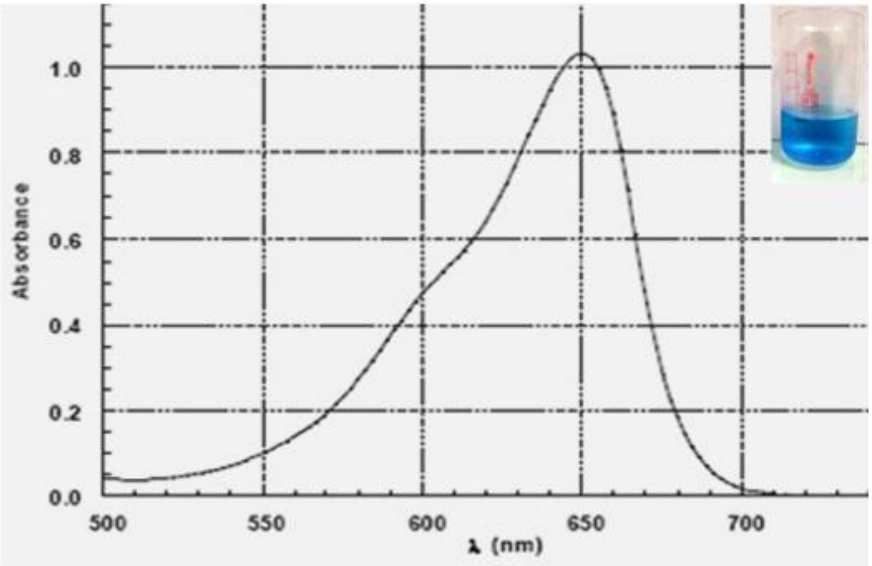

Figure 15. Spectrum UV-Vis of methylene blue

The electrocatalytic degradation activity of the electrodeposited ZnO-CeO_2 and ZnO-Cu_2O electrodes was examined. Generally, in the direct electrocatalytic degradation of organic pollutants, the organic molecules are oxidized on the electrode surface by the adsorbed •OH radicals electrogenerated from the water discharge.

The solution contained 20 mg/L MB + 2% NaCl « as electrolyte support » aqueous solution. The same electrochemical setup described previously was used, where ZnO and its nanocomposites thin films were used as anode electrode.

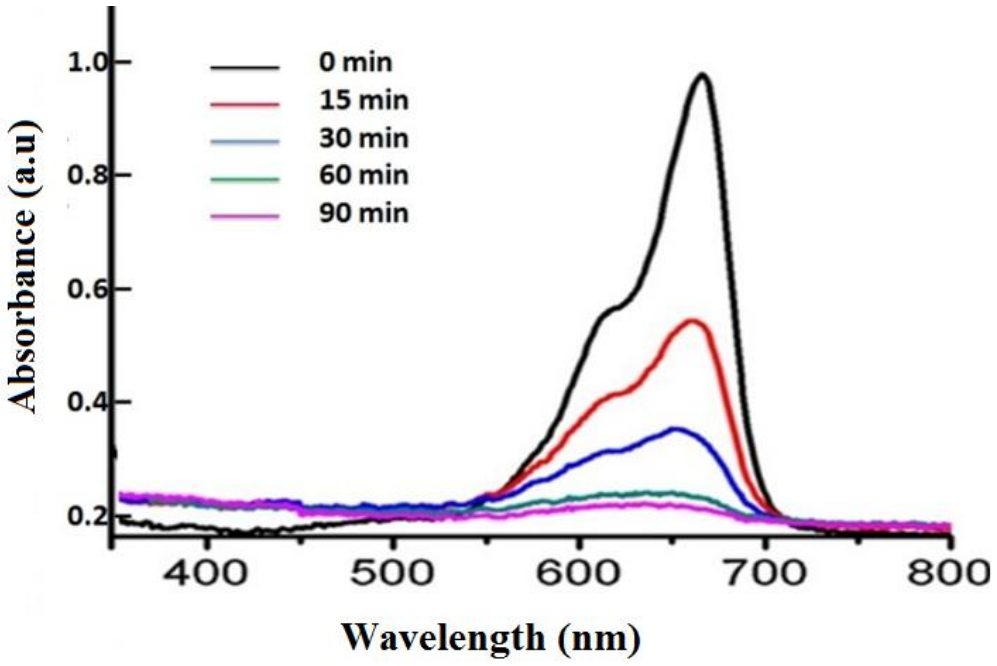

Figure 16. UV spectra of the electrolyte at some given electrolysis time

Fig.13 showed the UV–Vis absorption spectrum of an aqueous solution containing MB, and NaCl after different electrocatalytic durations.

As shown in the figure, the MB concentration decreases with the reaction time, and no new absorption bands appear in the visible region, indicating the destruction of the conjugated and chromophoric groups. Over 78% of MB was degraded within 90 min, suggesting a good catalytic property of the ZnO-Cu_2O nanocomposite film.

The periodic analysis of the chemical oxygen demand "COD" were carried out during electrolysis to determine the kinetics of degradation of MB on the three above-mentioned electrodes.

Table.3 showed the evolution of the percentage of COD according to the time of electrolysis.

Table 3. Variation of % COD during the degradation of MB.

Time (min)	% COD « ZnO/Ti »	% COD « ZnO-CeO_2/Ti »	% COD « ZnO-Cu_2O/Ti »
0	0	0	0
15	0.55	17.82	27.05
30	6.27	21.11	40.56
60	14.85	33.04	53.65
90	21.32	52.17	78.11

In the case of ZnO-Cu_2O electrode, we had an important percentage of degradation in the first time of electrolysis. However, % COD remained very weak for duration of 15 minutes of electrolysis for the two other electrodes especially on ZnO electrode. For higher periods of degradation, the % COD of MB on ZnO-Cu_2O increased quickly. At the end of 90 minutes, we had the values of 21.32, 52.17 and 78.11 respectively for ZnO, ZnO-CeO_2 and ZnO-Cu_2O electrodes.

4. DISCUSSION

Electrodeposition of thin films of ZnO has been extensively studied in recent years include for example the work of Peulon and Lincot [27]. In general, it consists to hydroxide precursor ions electroreduction like the nitrate ions [28-35]. Therefore, for electrodeposited ZnO thin films, nitrate ions were used as precursor [36]. The choice of this precursor is simple and interesting as it avoids the use of a gas. The electrochemical mechanism of deposition includes two steps. The first one corresponds to the cathodic generation of hydroxyl OH^- ions by the reduction of NO_3^-:

$$NO_3^- + H_2O + 2\,e^- \rightarrow 2\,OH^- + NO_2$$

The second, which should be the reaction of the Zn^{2+} with the hydroxide ions to form the ZnO film on the substrate surface, is:

$$Zn^{2+} + 2\,OH^- \rightarrow ZnO + H_2O$$

In this work, we are mainly interested to the electrochemical growth of zinc oxide. Unlike other materials, the electrolytic growth of this material often involves significant problems [26]. The major diffraction peaks correspond to a hexagonal ZnO structure (wurtzite) for almost all samples.

Diffraction peaks due to the substrates also appear, unless the concentration of Zn^{2+} precursor is reduced to values as 0.1M. This indicates that the microstructure and morphological characteristics of growth of ZnO depends on several parameters. Generally, the study shows that the type of the substrate, applied current density and the concentration of zinc nitrate had a significant impact on morphology, the size of the crystallites and the direction of film growth, respectively. This result is in agreement with some previous works [26, 30, 37]. However, the control over morphology and size of ZnO presents a great challenge in realizing the design of novel functional devices such as anode electrode. This was our reason to use the nanocomposite materials, especially as the content in ZnO thin films decreased the room temperature resistivity of the deposited films [38], but in some cases the resistivity tend to increase for highly nanocomposites/doped films [39]. The cathodic electrodeposition of ZnO-CeO_2 used as anode electrode for the degradation of dye was confirmed by all analysis. ZnO always kept its hexagonal form and the films were textured and grow along the (010) plane. The surface of deposit presents an important network of cracks, which are characteristic of ceria. These cracks are associated with either the formation of gas bubbles, to the dehydration process itself or from the shearing stress between the substrate and the deposit. The second proposal remains most probable.

Ceria played an important role in the system ZnO-CeO_2. It had high activity, good stability and find application in the catalysis field. It had a fluorite structure whose cations can switch between +3 and +4 oxidation states and it had the ability to act as an oxygen buffer to adjust oxygen concentration at the catalyst surface under reaction condition [40]. The catalytic activity of composite electrode using MB « methylene blue » electro-oxidation as a test reaction was investigated. The second system synthesized was ZnO-Cu_2O nanocomposite. ZnO conserved its wurtzite crystallographic form. Homogeneous, dense and smooth films were obtained. The growth of ZnO were oriented toward the c axis « (010) plane ». Generally, this synthesis also gave satisfactory results. The system ZnO-Cu_2O used as anode electrode has been tested for the potentiometric degradation of MB in the order to test its catalytic efficiency towards the degradation of the dye.

5. CONCLUSIONS

In the present work, the adequate parameters for the cathodic electrodepotion of ZnO are studied. The current density and the concentration of bath played a significant role in the formation of the deposit. Its growth rate seems to evolve quickly to forming a film leading to the stabilization of the potential. Also, the cathodic deposition, on the stainless steel substrate, of the thin films of ZnO-CeO_2 and ZnO-Cu_2O was carried out. We showed that the form and the thickness of deposit increased with the density of current applied. The electrocatalytic propreties of deposits towards the degradation of MB were also studied. While, by coupling the COD measurement with UV-Vis analysis, we showed that the elaborated anodes especially ZnO-Cu_2O electrode « 78% of % COD » had an electrocatalytic capacity to mineralize organic pollutants.

ACKNOWLEDGMENTS
The authors would like to acknowledge the Microelectronic Materials and Nanosciences Institute of Provence, University of Toulon - UFR Sciences & Techniques- France, and Engineering and Materials Science Laboratory (LISM), UFR Sciences, University of Reims, France, for their contributions.

References

1. C.X. Shan, Z. Liu, Z.Z. Zhang, D.Z. Shen, S.K. Hark, *J. Phys. Chem*. B 110 (2006) 1117.
2. C.Klingshirn. *ChemPhysChem.* 8(2007) 782-803.
3. J. M. Spero, B. Devito, L. Theodore, Regulatory chemical handbook. CRC Press. (2000).
4. J. L. G. Fierro, *Metal Oxides: Chemistry & Applications*. CRC Press. (2006) 182.
5. J.L. Yang, S.J. An, W.I. Park, G.C. Yi, W. Choi, *Adv. Mater*. 16 (2004) 1661.
6. F. Xu, Z.-Y. Yuan, G.-H. Du, T.-Z. Ren, C. Bouvy, M. Halasa, B.-L. Su, *Nanotechnology*. 17 (2006) 588.
7. F. Xu, G.-H. Du, M. Halasa, B.-L. Su, *Chem. Phys. Lett.* 426 (2006) 129.
8. B. Pal, M. Sharon, *Mater. Chem. Phys*. 76 (2002) 82.
9. F. Peng, H. Wang, H. Yu, S. Chen, *Mater. Res. Bull.* 41 (2006) 2123.
10. D. C. Look. Materials Science and Engineering B 80, (2001) 383.
11. F. K. Shan and Y. S. Yu. *Journal of the European Ceramic Society* 24 (2004) 1869.
12. S .J. Kang , Y.H. Joung, D.H. Chang and K.W. Kim. *J Mater Sci: Mater Electron*. (2007) 647.
13. J.H. Lee, K.H. Ko, B.O. Park, *J. Cryst. Growth*. 247 (2003) 119.
14. X. Chen, W. Guan, G. Fang, X.Z. Zhao, *Appl. Surf. Sci*. 252 (2005) 1561.
15. S.Y. Lee, E.S. Shim, H.S. Kang, S.S. Pang, J.S.Kang, *Thin Solid Films*. 473 (2005) 31.
16. E.Fortunato, T.P. Barquinha, A. Pimentel, A.Goncalves, A. Marques, L. Pereira, R. Martins, *Thin Solid Films*. 487 (2005) 205.
17. E. Hosono, S. Fujihara, T. Kimura, *Electrochem. Solid State Lett*. 7 (2004) C49.
18. D. Hariskos, S. Spiering, M. Powalla, *Thin Solid Films*. 480 (2005) 99.
19. D. Lincot, *Thin Solid Films*. 487 (2005) 40.
20. T. Mahalingham, V.S. John, M. Raja, Y.K. Su, P.J. Sebastian, *Sol. Energy Mater. Sol. Cells* . 88 (2005) 227.
21. J.S. Wellings, N.B. Chaure, S.N. Heavens, I.M. Dharmadasa. *Thin Solid Films*. 516 (2008)3893-3898
22. R.K. Pandey, S.N. Sahn, S. Chandra. Handbook of semiconductor electrodeposition. New York: Marcel Dekker. 53(1996) 105.
23. B.D. Cullity, Elements of X-ray Diffraction, 2nd ednR, Addison Wesley. Reading. MA (1978).
24. H.Y. Chang, H.I. Chen, *J. Cryst. Growth*. 283 (2005) 457.
25. J. Creus, F. Brezault, C. Rébéré, M. Gadouleau, *Surf. Coat. Technol.* 200 (2006) 4636.
26. J. Dini. Electrodeposition, Noyes Publication. Park Ridge. New Jersey. D55 (1992) 671.
27. S.Peulon, D.Lincot. *Adv. Mater*. 8 (1996) 166.
28. M.Izaki, T. Omi . *Appl. Phys. Lett*. 68 (1996) 2439.
29. M.Izaki, T.Omi *J. Electrochem. Soc*. 144 (1997) 1949.
30. J.Katayama, M. zaki *J. Appl. Electrochem*. 30 (2000) 855.
31. T.Yoshida, S.Ide, T.Sigiura, H.Minoura *Trans. Mater. Res. Soc. Jap*. 25 (2000) 1111.
32. T.Yoshida, D.Komatsu, N.Shimokawa, H.Minoura. *Thin Solid Films*. 166 (2004) 451-452.
33. J.Lee, Y.Tak . *Electrochem.Commun*. 2 (2000) 765.
34. E.A.Dalchiele, P.Giorgi, R.E. Marotti, F. Martin, J.R.Ramos-Barrado, R.Ayouci, D. Leinen *Sol. Energy Mater. Sol. Cells.* 70 (2001) 245.
35. R.E.Marotti,D.N.Guerra, C.Bello, G.Machado, E.A.,Dalchiele. *Sol. Energy Mater. Sol. Cells*. 82 (2004) 85.

36. Q. P.Chen, M. Z.Xue, Q. R. Sheng, Y. G.Liu, Z. F. Ma *Electrochem. Soli.-State. Ett*. 9 (2006) C558.
37. Z. Messaï, Z. Ouennoughi, T. Devers, T. Mouet, V. Harel, K. Konstantinov, N. Bouguechal, *Applied Surface Science*.257 (2010) 616.
38. I. Shih, C.X. Qiu, *J. Appl. Phys*. 58 (1985) 2400.
39. A. Maldonado, M. de la Luz Olvera, S. Tirado Guerra, R. Asomoza, *Sol. Energy Mater. Sol. Cells*. 82 (2004) 75.
40. S. Deshpand, S. Patil, S.V.Kuchibhatla, S. Seal. *Appl. Phys. Lett*. 87(2005) 133113.